SnT 2021
CTBT: SCIENCE AND TECHNOLOGY CONFERENCE

CTBTO
PREPARATORY COMMISSION

Use of small-aperture, near-source seismoacoustic arrays in characterizing low-yield chemical explosive sources

H.K.C. Perry, N. Ackerley, J. Morawetz, D. McCormack, R. van Brabant

P2.3-671

POSTER

Natural Resources Canada
Ressources naturelles Canada

Canada

Use of small-aperture, near-source seismoacoustic arrays in characterizing low-yield chemical explosive sources

H.K.C. Perry, N. Ackerley, J. Morawetz, D. McCormack, R. van Brabant

ABSTRACT

As part of a broader study on detecting and characterizing explosions in urban areas, we have studied signals from a range of industrial explosive sources at ranges less than 100 kilometres. We deployed two six-node, small-aperture (300 m) seismoacoustic arrays near Labrador City and Ottawa, Canada, over month-long periods. Using an empirical approach, we develop amplitude and period scaling relationships for estimating yield at distances 3-70 km using ground truth event details (location, explosive yield) provided by mine and quarry operators. The explosive sources are ripple-fire blasts with durations of 5-30 seconds. Reported origin times are generally accurate to within a few seconds. Blast yields range from 3-1000 tonnes of TNT equivalent and the associated seismic Nuttli magnitudes range from 1.3-3.2 M_N. We show that seismic and acoustic data are complementary and, when combined, result in improved blast characterisation: seismic data provides more stable constraints on yield estimates, while infrasound provides better constraints on location.

Use of small-aperture, near-source seismoacoustic arrays in characterizing low-yield chemical explosive sources

H.K.C. Perry, N. Ackerley, J. Morawetz, D. McCormack, R. van Brabant

CTBTO
PREPARATORY COMMISSION

INTRODUCTION

We investigate the rapid detection and characterization of explosions using rapid response deployable instrument kits. Small-aperture (300m), seismoacoustic arrays were deployed in two regions of Canada to characterize yield, predominant period and event location/azimuth from ripple-fire quarry blasting events at distances below 100km. **Deployment 1** took place in a remote region near Labrador City, and **Deployment 2**, near the urban centre of Ottawa. Data recorded by collocated accelerometers and microbarometers enable estimation of the explosive yield and blast location. The array station quality and performance are assessed and blast events of varying explosive yield and epicentral distance are studied. We use a beamforming method on the infrasound recordings to estimate the azimuth and location of the recorded blasts, and assess the predominant period of explosions of various yields.

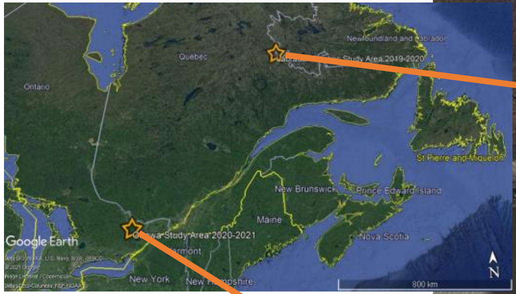

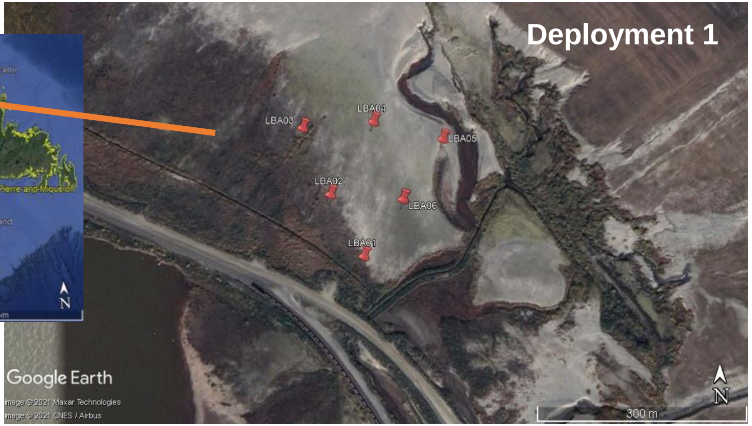

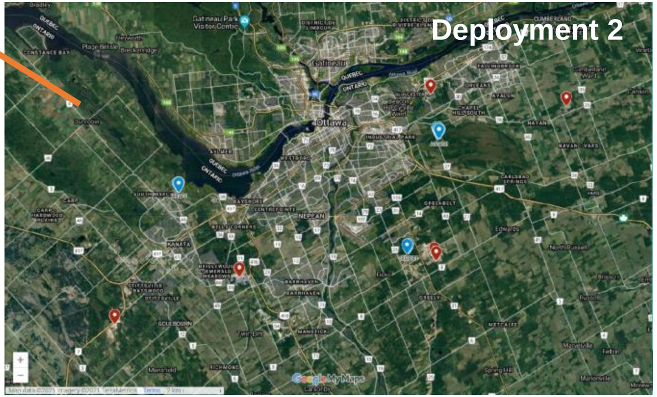

SnT 2021
CTBT: SCIENCE AND TECHNOLOGY CONFERENCE

Poster No.: P2.3-671

Use of small-aperture, near-source seismoacoustic arrays in characterizing low-yield chemical explosive sources

H.K.C. Perry, N. Ackerley, J. Morawetz, D. McCormack, R. van Brabant

CTBTO
PREPARATORY COMMISSION

METHODS

Dataset and Instruments

1. Blast source Open-pit quarry ripple-fire blasting consisting of a suite of detonations spaced milliseconds apart, for a total duration of 5-30 seconds. The seismoacoustic signal and noise windows analyzed are of equal length and are frequency-dependent.

2. Ground Truth Quantity and distribution of explosive, location, and approximate timing provided by quarries. Ottawa blasts have reported explosive yields 0.8-30 tonnes. Labrador blasts have reported yields 11-1000 tonnes. Explosive yield data used to calibrate seismic and infrasound amplitude and predominant period.

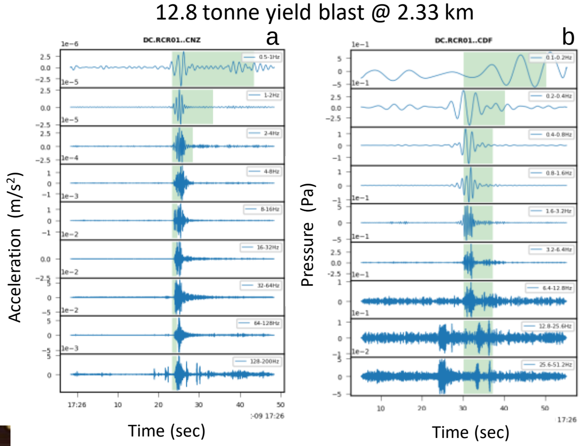

Fig 2 (a) Vertical acceleration (m/s2) at DC.RCR01.CNZ, and (b) infrasound signal (Pa) at DC.RCR01.CDF filtered over narrow frequency bands for a blast of 12.8 tonnes at the Navan Quarry, at an epicentral distance of 2.33km. The optimal signal-to-noise (SNR) is ~0.5-64 Hz for the seismic signal and ~0.4-6.4 Hz for the infrasound signal.

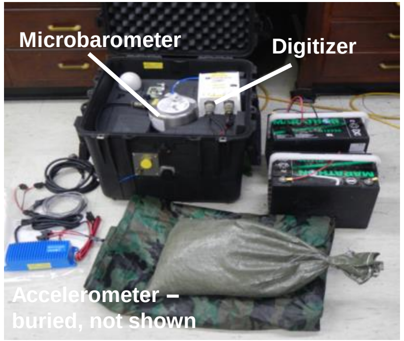

Fig 1 Instrumentation: 6-node seismoacoustic arrays. Each array node is equipped with an accelerometer, microbarometer, digitizer, GPS antenna, 4 permeable hoses, 2 marine batteries, insulated pelican case.

Detection Thresholds and SNR

Using the small-aperture arrays, blasts of 3-6 tonnes (M_N~=1.8) with SNR >=2 are detected from the background noise at distances 2-40km.

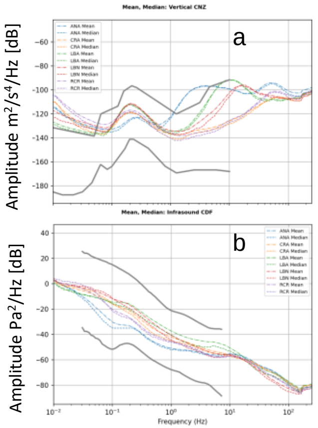

Fig 3 (a) Seismic and (b) acoustic ambient noise for arrays DC.LBA, DC.LBN, DC.ANA, DC.RCR, DC.CRA (medians and means over 16-50 days, depending on deployment), low and high noise models (seismic: Peterson, 1993 [1]; acoustic: Bowman, 2005 [2])

Fig 4 Operating range diagrams [3] for infrasound (a) and seismic (b) showing ambient noise levels and recorded blast signals from Ottawa quarry blasts.

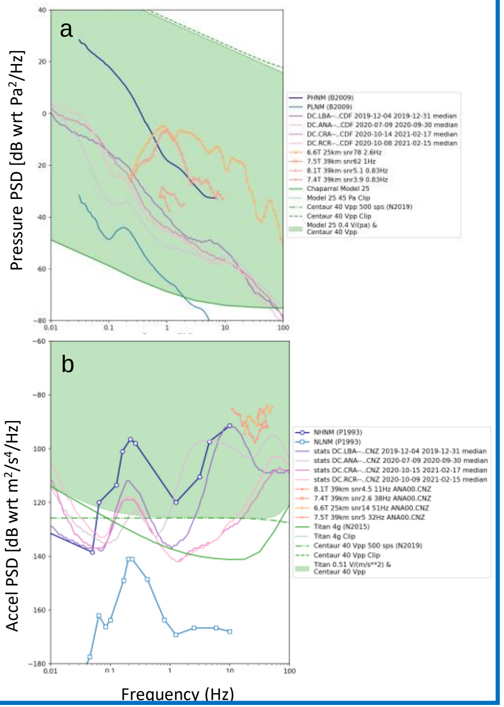

Use of small-aperture, near-source seismoacoustic arrays in characterizing low-yield chemical explosive sources

H.K.C. Perry, N. Ackerley, J. Morawetz, D. McCormack, R. van Brabant

METHODS

Array geometry and transfer function

Waveforms at array nodes are approximately identical, but separated by a discrete time shift, which is determined through cross-correlation. The stacked and time-shifted signal is scaled by a factor of N, where N is the number of nodes. Assuming that noise is truly random, the sum of N normal distributions increases the standard deviation by a factor of ΣN. The overall SNR gain is $N/\sqrt{N} = \sqrt{N}$ [4]. **Fig 5** illustrates the beamformed infrasound waveforms from DC.ANA for a blast on July 23, 2020.

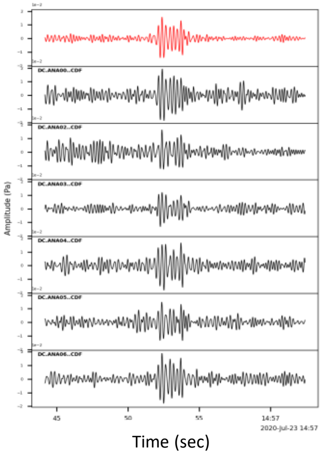

Fig 5 Infrasound stream of six 3.2-6.4 Hz bandpass-filtered and time-shifted waveforms recorded at DC.ANA (epicentral distance 12.5 km) for the July 23, 14:57 2020 4,860 kg explosive yield blast. Stacked waveform is shown in red

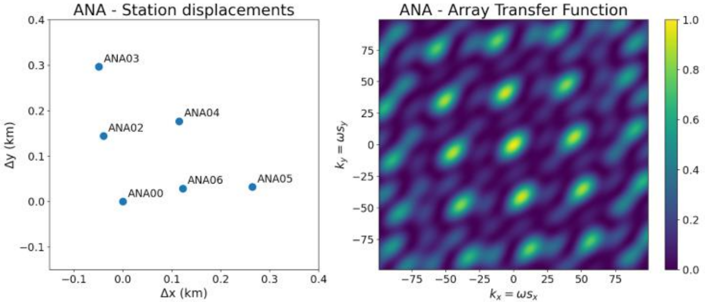

Fig 6 Station displacements and array transfer function (ATF) describing sensitivity and resolution of the ANA array for acoustic signals with different frequency contents and slownesses. Frequency band is 3.2-6.4 Hz. ATF values of 1 show no SNR improvement through stacking, while components near 0 show best SNR improvement.

Source characterization

1. Signal Amplitude and Predominant Period To evaluate blast energy at the source, we calculate the Fourier amplitude spectrum for a time window around each blast. SNR based on signal and noise windows of equal length (frequency-dependent). Frequency band centres are logarithmically-spaced, with 24 frequencies per decade. The frequency corners are set as 1/2 octave bands around the centres.

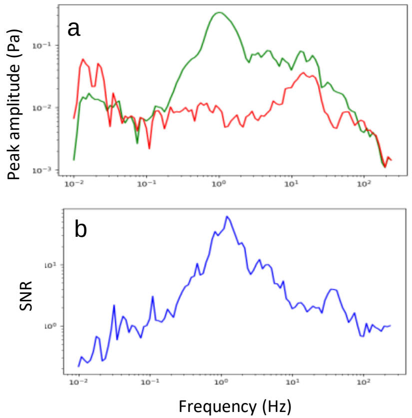

Fig 7 . (a) Sample spectrum from the quarry blast on September 8, 2020. Amplitude on the y-axis is maximum signal amplitude where the SNR>=2. The amplitude spectra for the signal (green) and noise (red) windows are overlain, (b) the SNR of this event over the frequency band of interest. The blast signal is detectable in a rather narrow band between 0.5-5Hz. Although various signal amplitude maxima may occur, the only reliably detectable maximum signal amplitude is that with SNR>=2.

2. Amplitude scaling for explosive yield In explosions, energy (E) is directly proportional to the explosive yield. Measured acceleration amplitudes are scaled to a reference yield (E_0), specifically the blast of maximum yield in the GT dataset, to facilitate comparison between blasts of varying yield and distance. Measured amplitudes are scaled to E_0 where:

$A' = A * \left(\frac{E_0}{E}\right)^{2/3}$ and E_0 *is* 10^5 kg.

SnT 2021
CTBT: SCIENCE AND TECHNOLOGY CONFERENCE

Poster No.: P2.3-671

Use of small-aperture, near-source seismoacoustic arrays in characterizing low-yield chemical explosive sources

H.K.C. Perry, N. Ackerley, J. Morawetz, D. McCormack, R. van Brabant

CTBTO
PREPARATORY COMMISSION

RESULTS

Predominant Period and explosive yield

Predominant period of blasts ranging from ~3-1000 tonnes from infrasound and seismic at DC.RCR01.{CDF,CNZ}. Acoustic blast recordings suggest a predominant period of ~1 sec (**Fig 9a**) across the range of reported yields, while the seismic recordings suggest a predominant period dependence on explosive yield: smaller blasts with explosive yields 3-30 tonnes suggest predominant periods of ~0.02 sec and larger blasts of yield 30-1000 tonnes show predominant periods near 0.1 sec (**Fig 9b**).

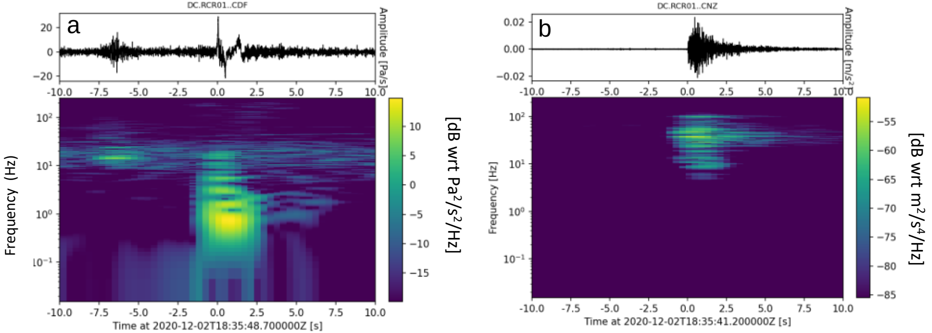

Fig 8 Spectrogram of infrasound recorded at DC.RCR01.{CDF,CNZ} for a blast of yield 5.8 tonnes at 2.8 km epicentral distance.

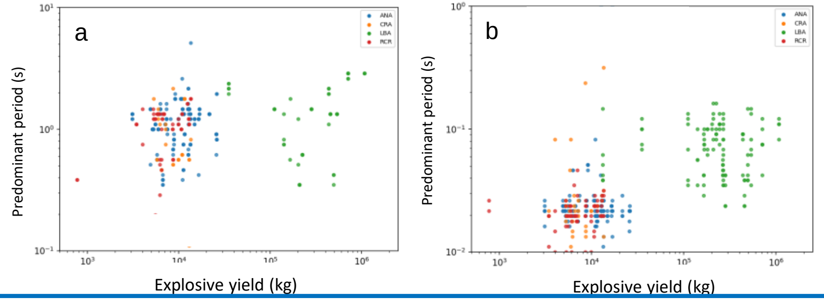

Fig 9 (a) Acoustic predominant period and (b) seismic predominant period as a function of reported explosive yield for the suite of ground truth blasts. Predominant period determined from Fourier amplitude spectra from blasts of SNR>=2.

Attenuation with distance

Fig 10 Scaled seismic amplitude vs. distance at frequency bands: 0.5-1 Hz, 4-8 Hz, 16-32 Hz,128-200 Hz. Acceleration amplitudes are scaled to $A' = A * \left(\frac{E_0}{E}\right)^{\frac{2}{3}}$ for reported yields at various distances.

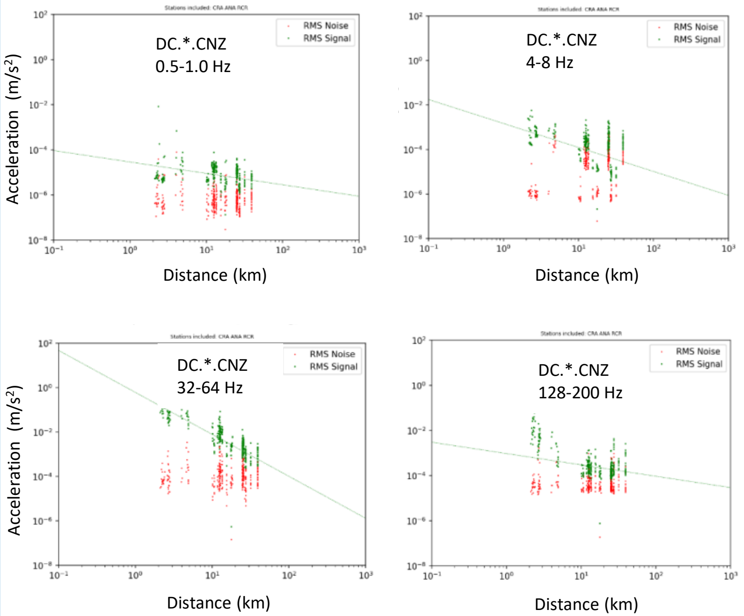

Disclaimer: The views expressed on this poster are those of the author and do not necessarily reflect the view of the CTBTO

Spectrogram of infrasound recorded at ANA00.CDF

SnT 2021
CTBT: SCIENCE AND TECHNOLOGY CONFERENCE

Poster No.: P2.3-671

Use of small-aperture, near-source seismoacoustic arrays in characterizing low-yield chemical explosive sources

H.K.C. Perry, N. Ackerley, J. Morawetz, D. McCormack, R. van Brabant

CTBTO PREPARATORY COMMISSION

RESULTS

Magnitude scaling for explosive yield

An empirical amplitude-yield relationship based on network magnitude and explosive yield (Y) is developed and compared with Nuttli's predicted yield vs. mbLg magnitude [5]. DC.LBA (red) and DC.ANA/RCR/CRA (blue) arrays recorded blasts at epicentral distances 3-70 km and explosive yields 3-1000 tonnes of TNT equivalent. M_N magnitudes are CN network magnitudes determined for event location.

$$mb(Lg) = 3.869 + 1.110 \log Y - 0.1(\log Y)\text{^}2$$

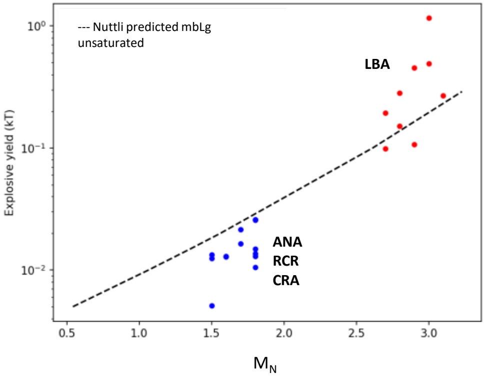

Fig 11 Explosive yield predicted by Nuttli relation (black dashed line) in kilotons vs. locally, CNSN-determined Nuttli solution magnitude for various ground-truth blast events near Ottawa (blue: ANA, CRA, RCR) and in Labrador (red: LBN, LBA). Error on event solution MN magnitudes is ~0.2 MN units, while error on explosive yield is unknown and based on the mass difference of explosive truck pre- and post-detonation. Note that MN magnitude (amplitude based on highest Lg peak) is compared here to mbLg magnitude (amplitude based on 3rd largest peak).

Event location and azimuth

Time shifts are computed using cross-correlation of array node waveforms, following the method of [6]. The time shift corresponding to the maximum cross-correlation is the optimal time shift. The time delay is the distance travelled (station separation projected on the direction of propagation) divided by the apparent velocity (the velocity observed at the Earth's surface). The slowness vector is parallel to the propagating wavefront, and its magnitude is the inverse of apparent velocity: $\tau_{ij} = \vec{r}_{ij} \cdot \vec{s}$.

τ_{ij} is the time shift of station j relative to i, $\vec{r}_{ij} = (x_{ij}, y_{ij})$ is the position vector of station j relative to i, and $\vec{s} = (s_x, s_y)$ is the slowness vector. There are two components of slowness, and 15 combinations in the array. Let R represent a 15x2 matrix, of relative position vectors for each of the station pairs. Let $\vec{T}$ represent a 15x1 matrix, whose entries are the associated time shifts. The matrix system of equations (represented by $R\vec{s} = \vec{T}$) is:

$$\begin{bmatrix} x_{12} & y_{12} \\ x_{13} & y_{13} \\ x_{14} & y_{14} \\ x_{15} & y_{15} \\ x_{16} & y_{16} \\ x_{23} & y_{23} \\ x_{24} & y_{24} \\ \vdots & \vdots \\ x_{56} & y_{56} \end{bmatrix} \begin{bmatrix} s_x \\ s_y \end{bmatrix} = \begin{bmatrix} \tau_{12} \\ \tau_{13} \\ \tau_{14} \\ \tau_{15} \\ \tau_{16} \\ \tau_{23} \\ \tau_{24} \\ \vdots \\ \tau_{56} \end{bmatrix}$$

The square matrix $R^T R$ is invertible, and solving this matrix system by multiplying both sides by $(R^T R)^{-1}$, provides the least squares estimate of the slowness [6]. The s_x and s_y components are determined, providing an azimuth θ.

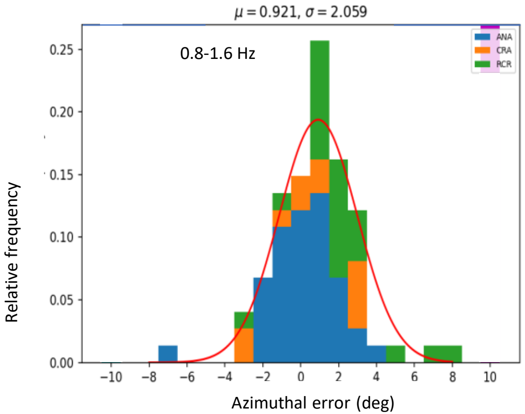

Azimuthal error (predicted - GT azimuth) from infrasound channels of 85 blast events recorded at Ottawa arrays ANA, CRA and RCR. Waveform coherence analysis was performed in the 0.8-1.6 Hz frequency passband. The azimuth error bins are colour-coded by array deployment. A gaussian fit is overlain in red. $\sigma = 2.06, \mu = 0.92$.

CONCLUSIONS

- Seismoacoustic arrays are used to constrain explosive yield at local distances. Seismic recordings are best used to constrain explosive yield, while acoustic data is used to constrain blast azimuth and direction. Seismic recordings provide the higher frequency signal (~0.02-0.01 sec), while infrasound captures the longer period ~1 sec signal.
- The 6-node 300-metre aperture seismoacoustic arrays deployed at epicentral distances ranging from 2-40 km are generally capable of detecting blasts as small as 3-6 tonnes (M_N~=1.8) with SNR >=2.
- The location method presented here for the infrasound array achieves ±2° azimuthal accuracy. If the source is posited to surround the array at 90°, the target may be constrained to a <4° box with 95% confidence. If the array is deployed within 5 km of the target, then the location accuracy is ±350 m with 95% confidence.

Future work:

- Compare seismic and acoustic attenuation
- Test the ability of two three-node seismoacoustic synchronous arrays to improve blast location at local distances

Use of small-aperture, near-source seismoacoustic arrays in characterizing low-yield chemical explosive sources

H.K.C. Perry, N. Ackerley, J. Morawetz, D. McCormack, R. van Brabant

REFERENCES

References

[1] Peterson, J.R., 1993, Observation and modeling of seismic background noise, United States Geological Survey, Open-File Report, No.OF 93-0322, 94p.
[2] Bowman, J. R., G. Shields, and M. S. O'Brien (2009), Infrasound station ambient noise estimates and models: 2003–2006 (erratum), paper presented at Infrasound Technology Workshop 2009, Univ. of Brasilia,
Brasilia.
[3] J. R. Evans, F. Followill, C. R. Hutt, R. P. Kromer, R. L. Nigbor, A. T. Ringler, J. M. Steim, E. Wielandt (2010). Method for Calculating Self-Noise Spectra and Operating Ranges for Seismographic Inertial Sensors and Recorders. *Seismological Research Letters*, 81 (4): 640–646. doi: https://doi.org/10.1785/gssrl.81.4.640
[4] Schweitzer, J., Fyen, J., Mykkeltveit, S., Gibbons, S. J., Kværna, T., K¨uhn, D., & Pirli, M. (2012). Seismic Arrays. New Manual of Seismological Observatory Practice, doi:10.2312/GFZ.NMSOP-2 ch9.
[5] Nuttli, O. W. (1986), Yield estimates of Nevada test site explosions obtained from seismic Lg waves, J. Geophys. Res., 91(B2), 2137– 2151, doi:10.1029/JB091iB02p02137.
[6] VanDecar, J. C., & Crosson, R. S. (1990). Determination of teleseismic relative phase arrival times using multi-channel cross-correlation and least squares, *Bulletin of the Seismological Society of America*, 80 (1): 150–169.